



Carbon – Science and Technology

ISSN 0974 – 0546

<http://www.applied-science-innovations.com>
ARTICLE

Received : 15/06/2013, Accepted : 12/08/2013

Special Section on Advanced (Non-Carbon) Materials

Effect of Temperature on Crystallite Size of Lanthanum Cerium Oxide (La₂Ce₂O₇) and its Optical Properties

Hozefa Tinwala ^(A,*), D. C. Shah ^(A) and Jyoti Menghani ^(B)

(A) Department of Applied Physics, Sardar Vallabhbhai National Institute of Technology, Surat - 395007, India.

(B) Department of Mechanical Engineering, Sardar Vallabhbhai National Institute of Technology, Surat - 395007, India.

***Corresponding Author** : Hozefa Tinwala, Tel: +91-8469691252.

The effect of the calcination process on the crystallite size and optical properties of Lanthanum Cerium Oxide (La₂Ce₂O₇) nanopowders synthesized using co-precipitation process were reported. X-ray diffraction analysis revealed that the synthesized nanopowders calcined at various temperatures have cubic fluorite phase. Thermal Gravimetric Analysis (TGA), X-ray Diffraction (XRD), Energy Dispersive Spectroscopy (EDS), Transmission Electron Microscopy (TEM), Laser Raman Spectroscopy, and UV-visible spectroscopy were utilized to characterize phase structure and morphology of the products.

Keywords : Crystallite Size, Co-precipitation Method, Thermal Properties, Optical Properties, Structural Properties.

Introduction : Rare earth doped ceria (REC) with a fluorite structure is used in wide applications such as solid oxide fuel cells (SOFC) due to its higher oxygen conductivity than that of ZrO₂ solid solution [1, 2, 3] and thermal barrier coatings [4, 5] due to its properties such as high melting point, low thermal conductivity, thermal expansion match with metallic substrate, no phase transformation between room temperature and operation temperature, chemical stability, good adherence to the metallic substrates and low sintering rate of the porous microstructure [6, 7]. Recent work done for the preparation of La₂Ce₂O₇ include the work by Benjaram et al. [8], Andrievskaya et al. [9], Cao et al. [10], Wang et al. [11]. Different methods were used in the preparation of La₂Ce₂O₇, such as hydrothermal method [11, 12], solid state method [13], cold

pressing and sintering [14], conventional co-precipitation method, [15]. Some of these methods are multistep [19], costly [14], and produces particles greater than nano-size [13, 14]. Long heating time is essential for solid state method, and cold pressing method, but results in formation of micron sized particles. In hydrothermal and conventional co-precipitation method, water is used as solvent for the synthesis of La₂Ce₂O₇, since water is used externally, results in the formation of hard agglomerates, due to hydrogen bonding. Thus by the elimination use of additional water, we can eliminate the formation of agglomerate [16].

Preparation of lanthanum cerium oxide nanopowders and studying its thermal and optical properties is a new research subject, practical

methods are still needed for synthesizing high quality ultrafine powders with required characteristics in terms of their size, uniformity, morphology, specific surface area and crystallinity. Very few techniques have been proposed to synthesize nano-sized lanthanum cerium oxide ($\text{La}_2\text{Ce}_2\text{O}_7$) with promising control of properties.

In the present study we report the effect of the calcination process on the crystallite size and optical properties of Lanthanum Cerium Oxide ($\text{La}_2\text{Ce}_2\text{O}_7$) nanopowders synthesized using co-precipitation process using Thermal Gravimetric Analysis (TGA), X-ray Diffraction (XRD), Energy Dispersive Spectroscopy (EDS), Transmission Electron Microscopy (TEM), Laser Raman Spectroscopy, and UV-visible spectroscopy.

Experimental Method : The co-precipitation process for making lanthanum cerium oxide $\text{La}_2\text{Ce}_2\text{O}_7$ was followed according to the work reported by Li *et al* [17]. The whole precipitation process was performed at room temperature. The cerium nitrate hexahydrate $\text{Ce}(\text{NO}_3)_3 \cdot 6\text{H}_2\text{O}$ (Spectrochem 99%) and lanthanum nitrate hexahydrate $\text{La}(\text{NO}_3)_3 \cdot 6\text{H}_2\text{O}$ (Loba Chemie 99 %) were used as source for synthesizing lanthanum cerium oxide $\text{La}_2\text{Ce}_2\text{O}_7$ powder. Triethylamine $(\text{C}_2\text{H}_5)_3\text{N}$ and ethanol were used as precipitant and solvent respectively. $\text{Ce}(\text{NO}_3)_3 \cdot 6\text{H}_2\text{O}$, $\text{La}(\text{NO}_3)_3 \cdot 6\text{H}_2\text{O}$ and $(\text{C}_2\text{H}_5)_3\text{N}$ were dissolved into the solvent separately. The final concentrations were 0.1 M for mixture of cerium nitrate and lanthanum nitrate solution and 0.4 M for triethylamine solution.

0.1 M mixture of cerium nitrate and lanthanum nitrate solution was mixed in a flask and titrated using 100 ml of 0.4 M triethylamine precipitant solution kept in another flask under mild stirring. The stirring was continued till the solution of cerium nitrate and lanthanum nitrate were empty, and solution was filtered by a suction filter using Whatman 42 (pore diameter 2.5 μm) filter paper. Precipitates was washed with solvent alcohol many times, then again washed with acetone to remove the remaining alcohol, unreacted triethylamine, and other byproduct. Then the

precipitates was dried for 24 hours, and calcined at different temperatures for 3 hours [16].

Thermogravimetric analysis (TGA, TGA-701, Rikagu, Japan), X-ray diffraction (XRD, Bruker X-ray diffractometer (D2 Phaser)), Transmission electron microscopy (TEM, Philips Tecnai 20, Holland), Electron dispersive spectroscopy (EDS), Raman Spectroscopy, and UV-visible spectroscopy were used as analytical tools to characterize the as prepared powder.

Results and Discussion :

Thermal Gravimetric Analysis (TGA) :

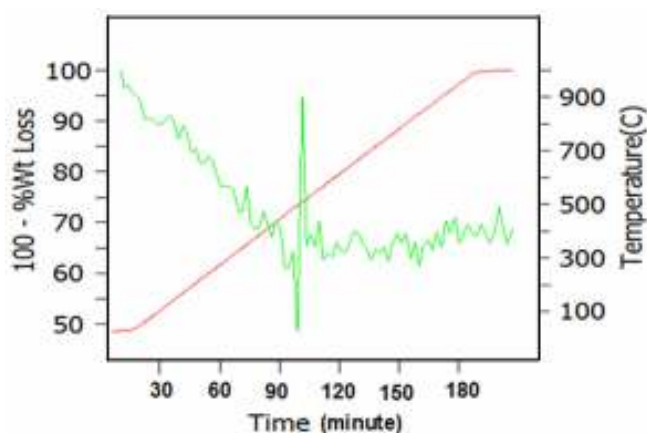


Figure (1) : Graph showing the weight loss of sample with respect to increment in temperature

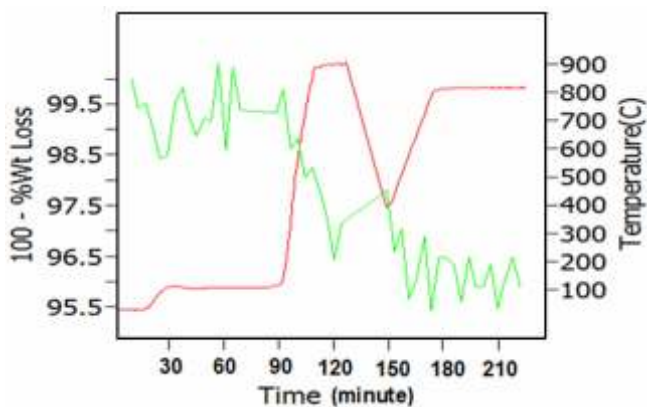


Figure (2) : Graph showing the weight loss of sample with respect to increment in temperature.

TGA Analysis was done using RIGAKU TGA-701, at SIC, Mechanical Engineering Department, SVNIT. Figure (1a) shows the graph of weight loss vs temperature. In this graph the weight of

the substance decreases up to around 500 °C, but after that there is zero or negligible weight loss. Which suggest that all the volatile material is removed around that temperature.

X-Ray Diffraction (XRD) Analysis : Bragg showed in 1913 that diffraction from a crystal is described by the equation now known as Bragg's law :

$$2 d_{(hkl)} \sin\theta = n\lambda \tag{1}$$

This equation allows one to measure the perpendicular distance (d_{hkl}) between imaginary planes which form parallel families and which intersect the repeating unit cell filled with atoms in a way described by the Miller indices (hkl). X rays of wavelength λ may be thought of as reflecting from these imaginary planes at the measurable angle θ , where n is the order, θ is one-half of the diffraction angle. A powder pattern therefore contains a set of diffraction peaks at 2θ positions that correspond to the interplanar spacings in the crystal [18].

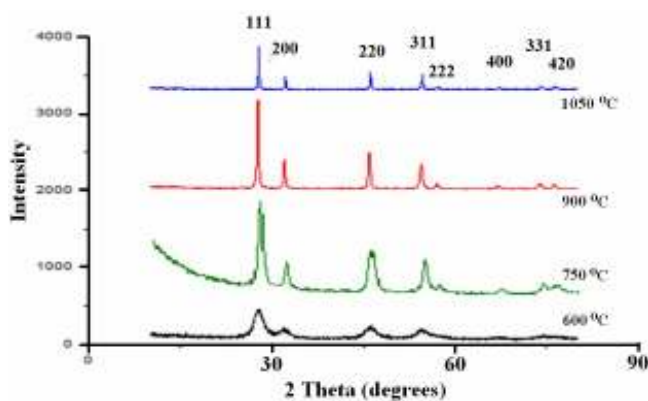


Figure (3) : XRD pattern for Naopowder Calcined at 600°C, 750°C, 900°C and 1050°C.

XRD Analysis was done using Bruker X-ray diffractometer (D2 Phaser), at K C Pattel Research and Development Center, Charotar University of Science and Technology (CHARUSAT). Figure (3) shows the XRD patterns of Lanthanum Cerium Oxide ($\text{La}_2\text{Ce}_2\text{O}_7$) nanopowders calcined at different temperatures. All the samples exhibit typical peaks corresponding to (1 1 1), (2 0 0), (2 2 0), (3 1 1) planes which are typical of face-centered cubic fluorite structure of CeO_2 [19]. The crystallite

sizes were estimated from the line broadening of the peak at (1 1 1) plane using Debye Scherrer equation [20].

$$D_{hkl} = \frac{\kappa\lambda}{\beta \cos \theta} \tag{2}$$

where D_{hkl} is the crystal size perpendicular to crystal face ($h k l$), K is constant, λ is 1.5406 Å and β is full width half maximum of the peak at (1 1 1) plane. The crystallite size increased with increasing calcinations temperature.

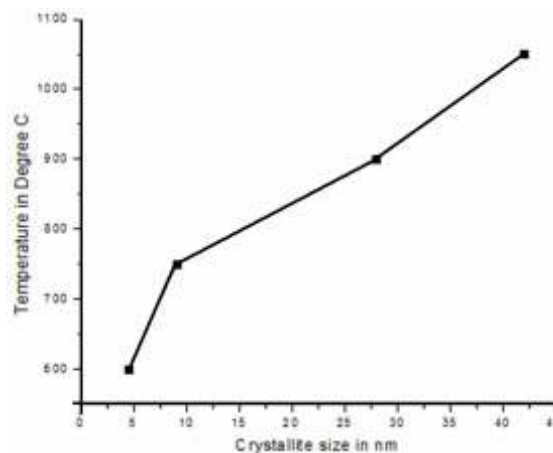


Figure (4) : Crystallite Size vs Temperature graph of Nanopowders

Detailed analysis indicates that XRD pattern match well with the standard cubic fluorite phase of CeO_2 . No evidence of $\text{La}_2\text{Ce}_2\text{O}_7$ pyrochlore phase (Fd3m) could be found. Furthermore, no peaks corresponding to the individual oxides (La_2O_3 .) were observed. This feature can be attributed to the formation of $\text{La}_2\text{Ce}_2\text{O}_7$ solid solution

Energy Dispersive Spectroscopy (EDS) : Elemental composition of Lanthanum Cerium Oxide ($\text{La}_2\text{Ce}_2\text{O}_7$) as observed from EDS is show in the table below :

Table (1) : Compositon of $\text{La}_2\text{Ce}_2\text{O}_7$ sample

Element	Weight %	Atomic %
O	16.98	64.08
La	41.36	17.97
Ce	41.66	17.95

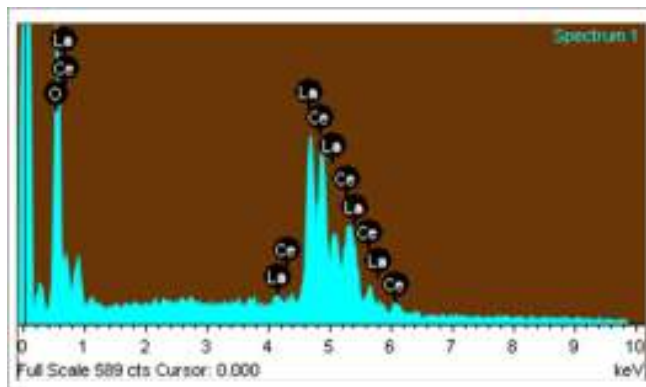


Figure (5) : EDS graph of sample

EDS measurements were carried out at M.S. University, Baroda. EDS measurements carried out on the as-prepared $\text{La}_2\text{Ce}_2\text{O}_7$ nanopowders indicates, the chemical composition of $\text{La}_2\text{Ce}_2\text{O}_7$ is closing to the stoichiometric composition of $\text{La}_2\text{Ce}_2\text{O}_7$.

Transmission Electron Microscopy (TEM) :

TEM analysis was done using Philips Tecnai 20, at SICART, Vallabh vidya nagar, Anand. The morphology, particle size and structure of the synthesized $\text{La}_2\text{Ce}_2\text{O}_7$ were illustrated by TEM. Figure (3a) and (b) illustrate the TEM images of the $\text{La}_2\text{Ce}_2\text{O}_7$ nanocrystals calcined at 900°C . The particles appear to possess the particle size 55 to 80 nm with cubic shape.

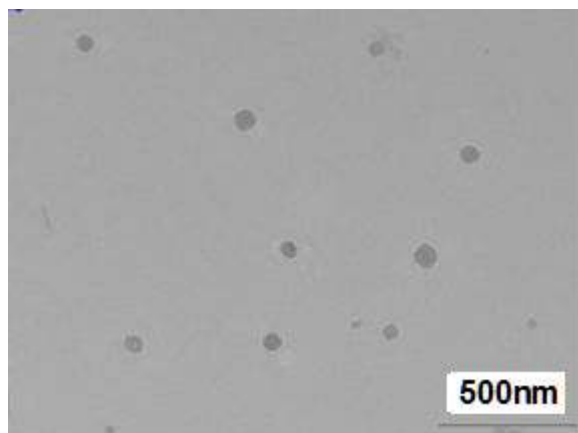


Figure (6) : TEM Image of Sample

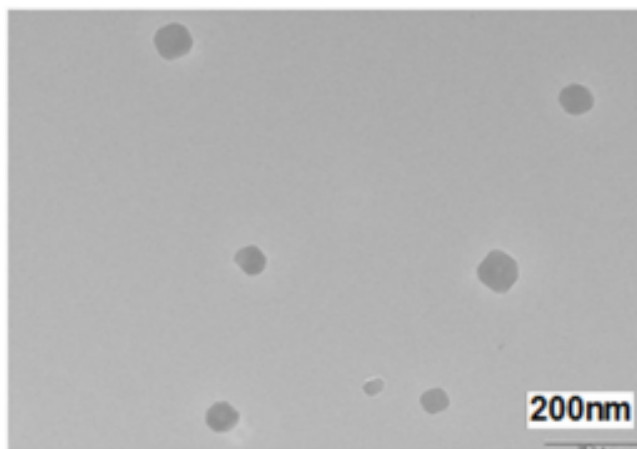
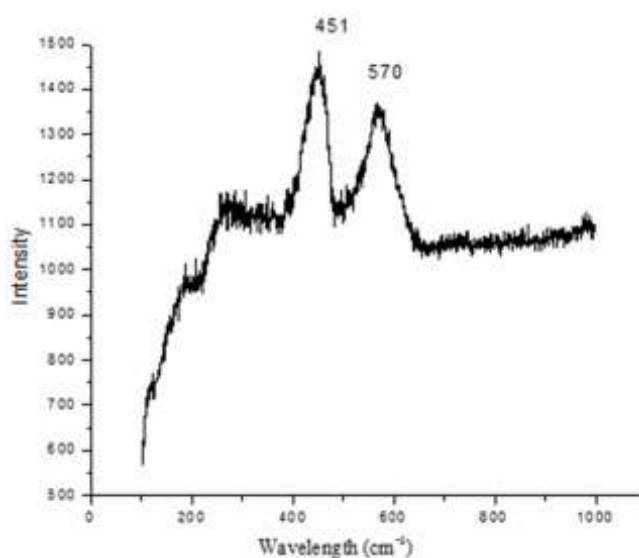


Figure (7) : TEM Image of Sample

Laser Raman Spectroscopic Analysis :

Figure (8) : Laser Raman Spectroscopic graph of Nanopowder Calcined at 900°C .

Laser Raman Spectroscopic Analysis was done using Ar-Laser; 4W power (all lines), Ramnor HG-2S Spectrometer, at IIT Bombay, The exposure time was 50 sec and the wavelength of laser source was 514.5 nm. Cubic fluorite structure metal dioxides have only a single allowed Raman mode, which has F_{2g} symmetry and can be viewed as a symmetric breathing mode of the O atoms around each cation. In above spectra two broad peaks are observed. 1st peak is at 451 cm^{-1} and 2nd peak is at 570 cm^{-1} . The 1st peak is CeO_2 peak it is shifted from 464.5 cm^{-1} to 451 cm^{-1} . This shifting is due to change in the M-O vibration frequency after incorporation of La in

CeO₂, which account for the difference in the ionic radius [21, 22, 23]. Vibrations are rapid for contracted lattice and slow down for expanded lattice so that band shifts to higher and lower wavenumbers, respectively. The peak at 570 cm⁻¹ is the new feature, and is due to the effect of dopant. Due to doping the O vacancies increases.

UV-visible Spectroscopic Analysis :

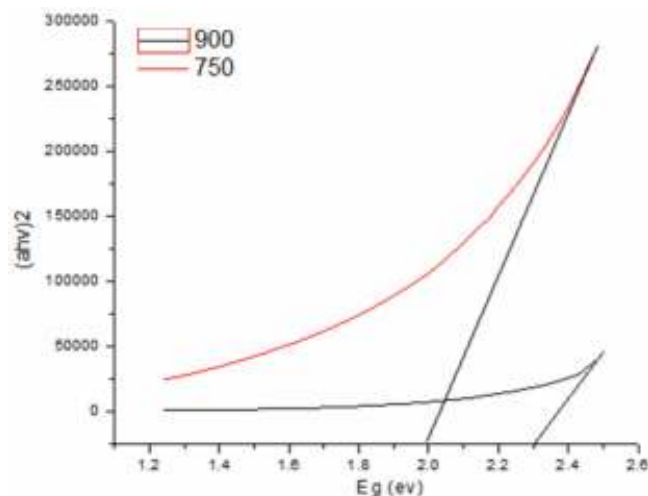


Figure (9) : Plot of $(\alpha hv)^2$ vs hv for 750°C and 900°C.

UV-Visible spectroscopic Analysis was done at Applied Physics Department, SVNIT. UV-Visible spectroscopy is frequently employed for band gap calculation. The band gap energy (E_g) is obtained from the intercept of the straight plot of $(\alpha hv)^2$ vs hv .

Here Absorption Coefficient α was calculated using the following equation :

$$\alpha = \frac{1}{d} \left(\frac{I}{I_0} \right) \quad (3)$$

where d is path length or thickness of powder film, I_0 is the intensity of light after reference glass plate, I is the transmitted intensity of light after placing powder film.

As observed from the UV-Visible graph, the bandgap of the synthesized material varies from 2.0 to 2.3 as the calcination temperature increases.

Conclusions : La₂Ce₂O₇ nanocrystals were produced via co-precipitation method. Thermo gravimetric analysis (TGA) of Nanoparticles in hydroxide form shows that weight loss is negligible as temperature increases above 500°C, and TGA of sample Calcined at 750°C also shows that the weight loss is negligible. From X-ray diffraction (XRD) Analysis of sample Calcined at 600°C, 750°C, 900°C and 1050°C standard cubic fluorite phase of Lanthanum Cerium Oxide (La₂Ce₂O₇) is observed. Electron Diffraction Spectroscopy (EDS) confirms La₂Ce₂O₇ phase. From Transmission Electron Microscope (TEM) morphology, particle size and structure of the synthesized La₂Ce₂O₇ was observed. Laser Raman Spectroscopy reveal the presence of vacant spaces due to doping of Lanthanum. And from UV-visible Spectroscopy it is observed that there is change in bandgap with increase in calcinations temperature. The products are cubic fluorite in structure. The nanoparticles have size in range 55-80 nm. This method is found to be simple and economical for the preparation of La₂Ce₂O₇ nanoparticles. XRD and TEM results suggest that the nanoparticles are cubic fluorite in structure. Laser Raman Spectroscopy reveals an extra peak at 570 nm.

References :

- [1] H. L. Tuller, A. S. Nowick, J. Doped Ceria as a Solid Oxide Electrolyte, *Electrochem. Soc.*, 122 (1975) 255-259.
- [2] J. S. Bae, W. K. Choo, C. H. Lee, The crystal structure of ionic conductor La_xCe_{1-x}O_{2-x/2}, *J. Eur. Ceram. Soc.* 24 (2004) 1291-94.
- [3] K. Eguchi, T. Setoguchi, T. Inoue, H. Arai, Electrical properties of ceria-based oxides and their application to solid oxide fuel cells, *Solid State Ionics* 52 (1992) 165-72.
- [4] W. Ma, S. K. Gong, H. B. Xu, X. Q. Cao, The Thermal Cycling Behavior of Lanthanum-Cerium Oxide Thermal Barrier Coating Prepared by EB-PVD, *Surf. Coat. Technol.* 200 (2006) 5113-18.
- [5] K. H. Kwak, B. C. Shim, S. M. Lee, Y. S. Oh, H. T. Kim, B. K. Jang, S. Kim, Formation and thermal properties of fluorite-pyrochlore composite structure in

- La₂(Zr_xCe_{1-x})₂O₇ oxide system Kwak, Mater. Lett 65 (2011) 2937-40.
- [6] P. Scardi, M. Leoni, F. Cemushi, A. Figari, Microstructure and heat transfer phenomena in ceramic thermal barrier coatings, J. Am. Ceram. Soc. 84 (2001), 827-35.
- [7] R. Vassen, F. Tietz, G. Kerkhoff, D. Stover, New Materials for Advanced Thermal Barrier Coatings, Proc. 6th Liege Conference. Materials for Advanced Power Engineering [C]. (1998) 1627-35.
- [8] M. Benjaram, M. Reddy, L. Katta, G. Thrimurthulu, Novel Nanocrystalline Ce_{1-x}La_xO_{2-δ} (x=0.2) Solid Solutions: Structural Characteristics and Catalytic Performance, Chem. Mater. 22 (2010) 467-75.
- [9] E. R. Andrievskaya, O. A. Kornienko, A. V. Sameljuk, A. Sayir, Phase relation studies in the CeO₂-La₂O₃ system at 1100-1500 °C, Eur. Ceram. Soc. 31 (2011) 1277-83.
- [10] X. Q. Cao, R. Vassen, W. Fischer, F. Tietz, W. Jungen, D. Stover, Adv. Mater, 15 (2003) 1438-42.
- [11] C. Wang, W. Huang, Y. Wang, Y. Cheng, B. Zou, X. Fan, J. Yang, X. Cao, Synthesis of monodispersed La₂Ce₂O₇ nanocrystals via hydrothermal method: A study of crystal growth and sintering behavior, Int. Journal of Refractory Metals and Hard Materials 31 (2012) 242-246.
- [12] F. Brisse, O. Knop, Pyrochlores. II. An investigation of La₂Ce₂O₇ by neutron diffraction, Can. J. Chem. 45(1967) 609.
- [13] W. Ma, S. Gong, H. Xu, X. Cao, The thermal cycling behavior of Lanthanum-cerium oxide thermal barrier coating prepared by EB-PVD, Surface & Coatings Technology 200 (2006) 5113-18.
- [14] T. Mori, J. Drennan, Y. Wang, J. Lee, J. Li, T. Ikegami, Electrolytic properties and nanostructural features in the La₂O₃-CeO₂ system, Journal of The Electrochemical Society, 150 (2003) A665-73.
- [15] S. Salehi, M. H. Fathi, Fabrication and characterization of sol-gel derived hydroxyapatite/zirconia composite nanopowders with various yttria contents, Ceram. Int. 36 (2010) 1659-67.
- [16] R. K. Pati, C. Ivan, Lee, K. J. Gaskell, S. H. Ehrman, Precipitation of Nanocrystalline CeO₂ Using Triethanolamine, Langmuir 25 (2009) 67-70.
- [17] J. G. Li, T. Ikegami, J. H. Lee, T. Mori, Characterization and sintering of nanocrystalline CeO₂ powders synthesized by a mimic alkoxide method, Acta Mater. 49 (2001) 419-426.
- [18] Parker, Greg. Encyclopedia of Materials : Science and Technology, 2001, pp. 9799-9809.
- [19] X. D. Zhou, W. Huebner, H. U. Anderson, Processing of Nanometer-scale CeO₂ Particles, Chem. Mater. 15 (2003) 378-82.
- [20] B. D. Cullity, S. R. Stock, Elements of X-Ray Diffraction, third ed., Prentice Hall, Upper Saddle River, NJ, 2001.
- [21] B. M. Reddy, P. Bharali, P. Saikia, A. Khan, S. Loidant, M. Muhler, W. Grunert, Hafnium Doped Ceria Nanocomposite Oxide as a Novel Redox Additive for Three-way Catalysts, The Journal of Physical Chemistry C. 111 (2007) 1878-81.
- [22] M. F. Luo, X. L. Yan, L. Y. Jin, M. He, Raman spectroscopic study on the structure in the surface and the bulk shell of CexPr_{1-x}O_{2-δ} mixed oxide, Journal of Physical Chemistry B 110 (2006) 13068-71.
- [23] B.M. Reddy, G. Thrimurthulu, I. Katta, Y. Yamada, S. E. Park, Structural characteristics and catalytic activity of nanocrystalline ceria-praseodymia solid solutions, Journal of Physical Chemistry C 113 (2009) 15882-90.